

1 **TICA: Transcriptional Interaction and Coregulation Analyzer**

2

3 Stefano Perna^{1,*}, Pietro Pinoli^{1,b}, Stefano Ceri^{1,c}, Limsoon Wong^{2,d}

4

5 ¹ *Dipartimento di Elettronica, Informazione e Bioingegneria, Politecnico di Milano, 20133 Milan,*
6 *Italy*

7 ² *School of Computing, National University of Singapore, Singapore 117417, Singapore*

8

9 * Corresponding author.

10 E-mail: stefano.perna@polimi.it (Perna S).

11

12 **Running title:** *Perna S et al / Transcriptional Interaction and Coregulation Analyzer*

13

14 ^aORCID: 0000-0002-2038-7121.

15 ^bORCID: 0000-0001-9786-2851.

16 ^cORCID: 0000-0003-0671-2415.

17 ^dORCID: 0000-0003-1241-5441.

18

19

20 Total No. of words: 6906.

21 Total No. of figures: 5.

22 Total No. of tables: 4.

23 Total No. of supplementary tables: 8.

24 Total No. of supplementary files: 2.

25

26 **Abstract**

27 Transcriptional regulation is critical to cellular processes of all organisms. Regulatory mechanisms
28 often involve more than one transcription factor (TF) from different families, binding together and
29 attaching to the DNA as a single complex. However, only a fraction of the regulatory partners of each
30 TF is currently known. In this paper, we present the Transcriptional Interaction and Coregulation
31 Analyzer (TICA), a novel methodology for predicting heterotypic physical interaction of TFs. TICA
32 employs a data-driven approach to infer interaction phenomena from chromatin immunoprecipitation
33 and sequencing (ChIP-seq) data. Its prediction rules are based on the distribution of minimal distance
34 couples of paired binding sites belonging to different TFs which are located closest to each other in
35 promoter regions. Notably, TICA uses only binding site information from input ChIP-seq
36 experiments, bypassing the need to do motif calling on sequencing data. We present our method and
37 test it on ENCODE ChIP-seq datasets, using three cell lines as reference including HepG2, GM12878,
38 and K562. TICA positive predictions on ENCODE ChIP-seq data are strongly enriched when
39 compared to protein complex (CORUM) and functional interaction (BioGRID) databases. We also
40 compare TICA against both motif/ChIP-seq based methods for physical TF–TF interaction prediction
41 and published literature. Based on our results, TICA offers significant specificity (average 0.902)
42 while maintaining a good recall (average 0.284) with respect to CORUM, providing a novel
43 technique for fast analysis of regulatory effect in cell lines. Furthermore, predictions by TICA are
44 complementary to other methods for TF–TF interaction prediction (in particular, TACO and
45 CENTDIST). Thus, combined application of these prediction tools results in much improved
46 sensitivity in detecting TF–TF interactions compared to TICA alone (sensitivity of 0.526 when
47 combining TICA with TACO and 0.585 when combining with CENTDIST) with little compromise in
48 specificity (specificity 0.760 when combining with TACO and 0.643 with CENTDIST). TICA is
49 publicly available at <http://geco.deib.polimi.it/tica/>.

50

51 **KEYWORDS:** Transcription factors; Coregulation; Protein–protein interactions; Machine learning;
52 Data-driven analysis

53

54 **Introduction**

55 Transcription factors (TFs) are proteins involved in the initiation and regulation of gene transcription.
56 DNA-binding domains present on TFs make them able to bind to specific DNA sequences, such as
57 promoter sequences near transcription start sites (TSSs). Some bound TFs help to form the
58 transcription initiation complex, while others bind distal regulatory regions to either stimulate or
59 repress transcription of the targeted genes [1]. Transcriptional regulation is the most common form of
60 gene control and the action of TFs allows for unique expression of each gene in different cell types
61 and/or during different stages of cell development [1].

62 Members of TF families often require some interactions with other members from the same or
63 even a different family [2]. These interactions can be of various nature, from protein dimerization and
64 concurrent DNA binding to recruitment or suppression of other TFs' binding in the proximity of a
65 DNA-binding domain or site [3,4]. Depending on the choice of partner, nature of the interaction, and
66 cellular context, each interactor triggers a series of regulatory events, thus leading to a particular
67 cellular fate [5]. The binding of TFs to their specific motifs in genomic regulatory regions has been
68 the focus of extensive study; given that only a limited amount of TFs can be encoded in a genome, let
69 alone be expressed at any given moment, combinatorial gene regulation strategies are required to
70 generate diverse expression patterns [6]. Nevertheless, only some combinatorial regulatory effects
71 are known, partially due to the intrinsic complexity of examining all combinations of a large number
72 of TFs and partially due to the many confounding effects that influence TF DNA-binding and
73 co-binding during *in vivo* confirmation experiments [7]. Thus computational methods provide a
74 powerful supplement to wet-lab experiments in discovering co-regulation phenomena.

75 In this paper, we present the Transcriptional Interaction and Coregulation Analyzer (TICA), a
76 computational method for *in silico* discovery of combinatorial TF interaction, based on ChIP-seq data.
77 The “interactions” considered in this study include direct binding between TFs, presence of TFs in the
78 same complex without direct contact between TFs, and blockage of another TF from binding its
79 cognate partners. All three cases mentioned above exhibit co-located peaks in the regulatory region(s)
80 of the cognate target genes of the TFs. Therefore, we look for significant co-located peaks in
81 ChIP-seq datasets for the TFs studied. It is of note that we do not attempt to distinguish between the
82 three kinds of aforementioned interactions or to decipher the regulatory effect of such interactions on
83 the expression of cognate target genes.

84 We implemented TICA using the genometric query language (GMQL) [8], a high-level,
85 interval-based query language for genomic datasets to support knowledge discovery across genomic
86 repositories. GMQL extends the set of relational algebra operators with domain-specific ones, such as
87 COVER, MAP, and JOIN, which were used to identify valid binding peaks and efficiently detect

88 region hits in the neighbourhood of TF binding sites (TFBSs) and TSSs. Python was used for
89 statistical testing (with modules pandas [9], NumPy [10], and scipy [11]). The TICA implementation
90 is accessible as a web service at <http://geco.deib.polimi.it/tica/>.

91

92 **Methods**

93 **Conceptual description**

94 TICA combines ChIP-seq peak datasets from a list of TFs in a single cell line and generates
95 interaction hypotheses, that is to say TF pairs that exhibit significant colocation based on
96 experimental data.

97 Our model was built based on the assumption that interacting TFs must be enriched in
98 co-locating peaks, and in the promoters of their cognate target genes, that is, if two binding sites from
99 two different TFs are in the promoter region of the same TSS, then there is a chance that they regulate
100 the expression of the splicing isoform defined by that TSS. Since physical interaction is directly
101 linked with coregulation [12], we assume that the more such binding sites of two different TFs are
102 found in the promoter region of the same TSS, the more likely these two TFs cooperate (or compete)
103 for the regulation of the same gene. Therefore, TFs are predicted to be interacting if the distance
104 distributions of the TF couples (defined as the number of base pairs intervening between the closest
105 ends of the regions that form the couples) is significantly skewed towards to 0 when compared to
106 those of random TF pairs.

107

108 **Data pre-processing**

109 *Transcription factor binding sites*

110 TICA requires genomic distances between TFBSs to be computed at precision levels close to
111 single-digit base pair lengths, so the preferred format for TICA input data is ENCODE narrowPeak
112 (<https://genome.ucsc.edu/FAQ/FAQformat.html#format12>). When multiple samples are given for a
113 single TF in a cell line, we consider as a binding site any region that is found in at least one of the
114 original samples after merging overlaps.

115 Since TICA can in principle use any point-source binding information, we expect that some
116 peaks in our input datasets could be artefacts or otherwise not significantly different from background
117 noise. In addition, experimental evidence has suggested that TFs exhibit multiple binding sites
118 clustered around target genes [13]. Based on the idea of binding clusters, we screen all binding events
119 in the input dataset and filter out the binding events that do not reach a minimum amount of same
120 binding events in a scanning area of 1 kb upstream and downstream of their boundary, which is set as
121 3 in our experiments.

122

123 *Transcription start sites*

124 Transcriptomics studies [14] suggest that not all spliced versions of a given gene are actively
125 transcribed in every single cell line. Thus, TICA uses a two-step filter to select only TSSs that are
126 active in a given cell. First, since TSSs that have a high amount of TF binding in their promoter region
127 are more likely to be transcribed [15], we consider a TSS to be actively transcribed when the number
128 of surrounding TFBSs is above a certain threshold, which is a parameter of the model. For our
129 experiments, we consider a nominal value of 50 TFBSs to be sufficient. Promoter regions are
130 standardized as spanning from $-N$ bases upstream to $+M$ downstream of the TSSs (also parameters of
131 the model; **Table 1**). Second, evidence for active transcription is given by the presence of certain
132 histone modifications upon or in the area surrounding a TSS, we thus use ChIP-seq broadPeak
133 sequencing data (for reasons discussed in [16]) of the histone marks. These include H3K36me3
134 (found on the gene body of actively-transcribed genes [17], H3K4me1 (found in enhancer regions of
135 actively-transcribed genes [18]), as well as H3K9ac and H3K4me3 (both found in promoter region of
136 actively-transcribed genes [19]). A TSS is considered actively transcribed if at least one nucleotide
137 base can be found in each of these regulatory regions with the relevant histone mark. GMQL queries
138 for TFBS and TSS filtering are presented in File S1.

139

140 **Minimal distance couple**

141 We define two binding sites \bar{x}_1 and \bar{x}_2 of two different TFs, TF₁ and TF₂, to be a minimal distance
142 couple (mindist couple) if:

$$d(\bar{x}_1, \bar{x}_2) = \min_{x_i \in T_1} d(x_i, \bar{x}_2)$$

AND

$$d(\bar{x}_1, \bar{x}_2) = \min_{x_j \in T_2} d(\bar{x}_1, x_j)$$

143 where T_1 and T_2 refer to the sets of all binding sites available for TF₁ and TF₂, respectively, and
144 $d(_, _)$ is the chromosome-wise base-pair distance on the genome (the distance between TFBSs on
145 different chromosomes is assumed to be infinite). We define d as the mindist couple distance, and we
146 observe that it is well defined for each mindist couple (due to the existence of the minimum of a finite
147 set of numbers). To account for the localized nature of genomic interactions, we impose an upper
148 bound on d , which equals to the sum of one standardized promoter length plus one standardized exon
149 length (Table 1).

150 To compute the mindist couple distances, first we merge the lists of binding sites (filtered as
151 described in Data pre-processing section) for the two TFs of interest, keeping track of the source.
152 Then for each of the sorted binding sites (henceforth *anchor*), we check if two conditions are met: (1)

153 at least one of the two adjacent binding sites belongs to a different (*i.e.*, the other) TF; and (2) the
154 distance from the anchor to at least one of the differently-labelled TFBS is below the aforementioned
155 upper bound. **Figure 1** exemplifies the process using synthetic data.

156

157 **Prediction algorithm**

158 TICA requires two conditions for TF–TF interaction prediction. First, if two TFs are physically
159 interacting while binding to the genome, their binding sites should generally be found close to each
160 other. If not, their binding sites should be spread widely from one another. Second, most of the TF
161 couples in a cell line are expected to be non-interacting [5]. Therefore, after pairing the closest
162 binding sites between two TFs, interactors should exhibit a distribution significantly skewed towards
163 0 with respect to random, non-interacting TF couples (**Figure 2** and **Figure 3**).

164 Following these assumptions, we developed a two-fold test based on mindist couple distribution
165 to predict interactions. Firstly, a deterministic rule excludes TF couples which do not present enough
166 biological information in the datasets. Then, a combination of statistical tests that aggregate
167 information from the distributions is evaluated to determine whether a couple is more skewed than
168 the typical distribution in the same cell line.

169

170 *Biological information thresholding*

171 The more couples are found to co-locate in the promoter region of the same TSSs, the more likely
172 they actually interact in order to regulate the same genes [20]. Hence, we hypothesize that TF pairs
173 that do not co-locate in a large enough number of sites are unlikely to be interactors; also, if too few
174 couples are found in promoters, the TFs are unlikely to be part of a regulatory module [21]. Therefore,
175 we only consider as valid those predictions where candidates have a high enough amount of mindist
176 couples, and for which the percentage of said couples that co-locate in the same promoter is also
177 sufficiently high. Both these minimum levels are parameters of the algorithm and can be tuned by the
178 users.

179

180 *Statistical tests*

181 Assuming two candidate TFs offer enough biological information, by pairing all their binding sites
182 we determine their observed distance distribution. To infer whether a physical interaction occurs, we
183 compute test statistics that describe the skewedness of the observed distribution towards zero. The
184 chosen test statistics are median, median absolute deviation (MAD), average, and the long (right) tail
185 size. Median, MAD, and average are well-known centrality measures, whereas the long tail size is to
186 the best of our knowledge a novel contribution to the field (described below).

187

188 *Right distribution tails*

189 The concept of *distribution right long tail* can roughly be identified as the points of said distribution
190 which are greater than or equal to a certain threshold value. The key observation is that if two TFs
191 frequently co-locate close to each another, the number of mindist couple that has a large intracouple
192 distance should be low. This is a complement of the reasoning of Jankowski and colleagues [22,23]:
193 physically interacting TFs show mindist couple distance distributions which are tightly packed
194 around low values, *e.g.*, Myc-associated factor X (MAX) and Myc (Figure 3), whereas randomly
195 picked TF couples give rise to distributions which are significantly more spread out, *e.g.*,
196 CCCTC-binding factor (CTCF) and Myc in Figure 2). In our work, we consider the 1000-bp mark as
197 the starting point for the right tail, whereas the 500-bp mark is more suited to the cases with a lower
198 number of couples available. An example of the shape and size of the right tail for distance
199 distributions is shown in **Figure 4**.

200

201 *P values and null hypotheses*

202 Each statistic is used to test whether or not a candidate couple is significantly different from the
203 respective null distribution. *P* value for these tests is defined as the fraction of points in the null
204 distribution corresponding to the respective test statistics which are closer to 0 in magnitude. Thus,
205 we reject a certain null hypothesis H_0 at *P* value threshold p^* (say, 0.05) for test statistic θ with
206 respect to TF_1 and TF_2 if and only if $\mathbf{P}(\theta_0 \leq \theta(TF_1, TF_2)) \leq p^*$, where \mathbf{P} is the empirical
207 frequency measure and θ_0 is a generic point in the null distribution generated by θ .

208 Briefly, we build null distributions for each cell line by randomly sampling candidate couples
209 from a list of background TFs, *i.e.*, those with a TFBS count between the top 10% and bottom 10%
210 marks after filtering (to remove the most extreme combinations) and extracting the mindist couples'
211 distance distribution (disregarding promoter colocation). We compute each of the four test statistics
212 on such distribution: each of these is a point of the corresponding null distribution to be used in the
213 final test. This process is repeated many times (usually at least 10,000), generating the required null
214 distributions.

215 TICA tests the aforementioned null hypothesis for a subset of the aforementioned test statistics
216 defined by the user and calls a candidate pair of TFs as interacting if and only if a minimum number
217 of such hypotheses (also defined by the user) is rejected in this way. When testing on 3 out of 4 of the
218 aforementioned statistics (baseline scenario), we selected a *P* value threshold of 0.20 for all tests
219 associated (Table 1) and detailed reasons for this lax choice are given in File S2.

220

221 **Validation**

222 To the best of our knowledge, there is no single gold standard for the evidence of physical interactions
223 and/or non-interactions. In particular, it is not clear how one should define a pair of TFs as
224 non-interacting, given that most databases report only positive cases and are potentially incomplete.
225 Nonetheless, two TFs that interact and have binding sites close to each other are expected to be part of
226 the same protein complex. Thus, a positive prediction that is confirmed by a protein complex
227 database is more likely to be correct with respect to one that isn't.

228 To investigate this, we confront our predictions with CORUM [24], a catalogue of protein
229 complexes in mammalian organisms derived experimentally; we use human core complexes database
230 released on July 2nd, 2017 (<http://mips.helmholtz-muenchen.de/corum/#download>). We also
231 compared our prediction with a curated list of human protein-protein interactions in BIOGRID [25]
232 as secondary evidence. Details are reported in File S2.

233 A pair of TFs can be considered as actually positive and supported by CORUM if its components
234 are mentioned together in at least one CORUM complex. We assume that if a certain TF is not
235 mentioned at all in the database then it is not an object of the involved study; therefore, all pairs
236 containing that TF are discarded from the set of predictions that are searched for in the database.
237 Finally, we define a pair of TF as negative if it is not positive and both its TFs cannot be discarded. We
238 also restrict our interactions to complexes/interactions that contain TFs only.

239 Given the actually positive and negative sets defined above, we compute the recall/sensitivity
240 and specificity measures, which remain invariant when the positive/negative proportion changes in
241 the test data. This is important since we do not have a clear idea of how such positive/negative
242 proportion changes when the databases get updated. We use the geometric mean performance
243 $GMP \stackrel{\text{def}}{=} \sqrt{RS}$ to combine recall and specificity, which works better when the positive:negative split
244 is unbalanced [26].

245 We also compute the enrichment ratio, defined as recall divided by (1- specificity). The higher
246 the enrichment, the more accurate we can expect the predictions to be. There are, however, some
247 caveats. First, CORUM is incomplete, so the observed recall may be lower than actual when a
248 predicted TF-TF interaction is co-operative or competitive in nature (hence not reported). Second,
249 CORUM also includes complexes that are not involved in gene transcription, so the observed
250 specificity may be lower than actual when a predicted non-interacting TF-TF pair is found as a
251 co-complex pair. At the same time, the observed recall may be higher than actual when some
252 predicted interacting pairs are actually non-interacting. However, since we restrict CORUM proteins
253 to TFs in this study, the latter situation is minimized.

254 Finally, direct literature investigation allows us to be much more specific about the nature and

255 contents of the evidence supporting a prediction. We perform manual investigation in published
256 studies and literature that support our positive predictions by searching on public interfaces such as
257 PubMed (<http://www.ncbi.nlm.nih.gov/pubmed/>) for published studies pertaining to a selected subset
258 of interactors. We mark as “confirmed” a positive prediction when there is evidence in the literature,
259 regardless of cell lines, that the two TFs physically bind to each other, bind to the same complex, or
260 there is a statement that they are co-factors or that they compete for the same co-factors or target
261 genes. As the process is time-consuming, we limit our manual checks only to a small subset of
262 predictions for each cell line (Table S1).

263

264 **Results**

265 **TICA parameters choice maximizes recall without sacrificing specificity**

266 We performed several computational experiments using TICA on human ChIP-seq data from various
267 immortalized cell lines to evaluate its performance. Three reference cell lines were tested, including
268 HepG2 (liver carcinoma), K562 (chronic myelogenous leukaemia), and GM12878 (healthy blood
269 cells). Data was downloaded from the ENCODE phase 2 (around 12% of samples) and 3 (around
270 88% of samples) repositories, using human genome assembly version 19 (hg19) as reference
271 alignment. **Table 2** reports the dataset cardinality for each cell line. We fitted our parameters using
272 datasets from HepG2, a cell line with abundance of ChIP-seq libraries available in ENCODE and of
273 gene expression [27], suitable for building null distributions and tuning parameters. Table 1 reports
274 threshold values chosen for each parameter, including the minimal number of minimal distance
275 couples (see Methods) and minimal percentage of TSS co-location. These values have been chosen to
276 maximize recall, since tuning has shown that this choice does not significantly impact specificity.

277 We investigated whether the parameters fitted on HepG2 provide good results on other cell lines
278 as well. To do this, we run TICA on two additional, well-studied cell lines (HEK293 and HeLa-S3)
279 using the HepG2 parameters and ENCODE phase 3 datasets. A good performance was achieved on
280 HeLa-S3 with respect to both databases (3% of possible interactors reported as a complex in CORUM
281 and 8% as a PPI in BioGRID), on par with other cell lines (Table S2). For HEK293, we found out that
282 only 13 TFs available in our ENCODE datasets are found in CORUM; on the other hand, while more
283 than 150 ENCODE TFs are found in BioGRID, only 67 out of ca. 13,000 possible pairs are reported
284 as PPIs (0.5%). We thus conclude that the reference datasets are not adequate enough to be used in
285 validation for HEK293.

286

287

288 **Type and number of TICA predictions**

289 We compiled lists of candidate and background TFs for each cell line (Table S3). Candidate pairs are
290 compiled using TFs for which narrowPeak data in the corresponding cell line is available in
291 ENCODE at the time of writing. Due to the way binding sites are matched by TICA (see Methods),
292 we cannot predict homotypic TF–TF interactions (*i.e.*, interactions between TFs of the same kind).
293 Thus, given N TFs for which experimental data are available and assuming the symmetry of
294 interaction phenomena, we have up to $N(N-1)/2$ possible tests. We computed all the statistics listed in
295 Methods, requiring at least three of the corresponding tests to be rejected for a prediction to be called
296 positive. Detailed listings of candidates and predicted interactions obtained by running TICA on all
297 cell lines using the default parameters are reported in Table S4.

298

299 **Enrichment with respect to CORUM is above 1 for all cell lines**

300 Using FANTOM TF list for humans [28], we found 535 TFs out of 3601 proteins in CORUM
301 complexes and 5709 couples of TF–TF interactions. Observing the confusion matrices with respect to
302 CORUM, we note that the number of true negatives (*e.g.*, 1079 in HepG2 data) is much higher than
303 that of false positives (293), and even one to two orders of magnitude higher than that of false
304 negatives (40), indicating that TICA shows very high specificity across all test scenarios.

305 In Table S2, we report recall, specificity, and enrichment analysis of TICA predictions with
306 respect to CORUM and for all three cell lines and their intersections. We observe that enrichment
307 ratio remains well above 1 for all test scenarios (minimum at 1.505, and almost always above 2.000).

308 We expect many of our predicted positives that could not be verified using CORUM (*i.e.*, the
309 presumed false positives) to be real positives, which awaits biological validation. For instance, out of
310 the 42 (109 – 67) sampled positive predictions for HepG2 that were analyzed for CORUM (*i.e.*, both
311 TFs in each of these 42 couples were found in CORUM), 35 (32% of the total) are not reported to be
312 co-complexed in CORUM (Table S5). Notably, 21 of these 35 predicted interactions have literature
313 support. Thus, 32% of the current presumed false positives with respect to CORUM might turn out to
314 be true positives. For K562, a similar calculation suggests 45 (54.2% of the total) of the current
315 presumed false positives might turn out to be true positives.

316

317 **TICA predictions are confirmed by manual literature investigation**

318 We performed manual literature investigation of selected predictions in tumour cell lines (HepG2 and
319 K562) and classified the predictions according to whether they can be verified as positives or
320 negatives with respect to literature, as described in Methods. As shown in **Figure 5**, about half of the
321 predictions were confirmed in published literature. Notably, more than 50% of these prediction were
322 also confirmed in one of the two databases (CORUM and BioGRID), suggesting a strong biological

323 support for TICA predictions, irrespective of cell lines. A complete report of the literature
324 investigation is given in Table S1.

325

326 **Cross-cell validation in the three cell lines shows TFs predictions in healthy to be validated**

327 We then investigated the amount of overlap between the sets of predicted positive interactions in
328 different cell lines. To do so, we used the *Jaccard Coefficient*, defined as the ratio between the sizes of
329 the intersection and of the union of the two sets. Moreover, we compared a single cell line with the
330 combined predictions in the other two; when merging or intersecting predictions in different cells, we
331 only consider those where both TFs are shared between the target cell lines. As shown in **Table 3**,
332 GM12878 shares almost 50% of its positively-predicted interactions with HepG2 and the same with
333 K562. This is consistent with the fact that GM12878 is derived from a healthy donor, and hence its
334 TF–TF complexes should be basal in nature, unlike aberrant versions in tumour cell lines. 20% of
335 positive TF–TF interaction predictions in GM12878 (on common TFs) are shared across all the three
336 considered cell lines, further validating this hypothesis (Table S6).

337

338 **Comparison with other TF-TF interactions prediction methods**

339 To evaluate the improvement with respect to the state of art in TF–TF prediction, we compared TICA
340 with three other methods for TF interaction prediction. These include TACO that predicts
341 cell-specific TF dimers based on enrichment of motif complexes [23], CENTDIST that is a co-motif
342 scanning algorithm ranking co-TF motifs based on their distribution around ChIP-seq peaks [29], and
343 a computational method based on nonnegative matrix factorization (NMF) [30]. Results are tabulated
344 in **Table 4**.

345 Using TACO, Jankowski et al. reported the top 10 best ranking predicted motif dimers using
346 ChIP-seq data on cell line K562 (*ibidem*, figure 4, page 6) [23]. We compiled the list of all TFs
347 belonging to these dimers and intersected it with data available in ENCODE. This resulted into 28
348 relevant TFs and 378 candidate TF pairs. Data for these pairs was extracted and fed to TICA. The
349 resulting predictions were compared with TACO’s original dimers. Note that if a TF pair is not
350 reported in the aforementioned dimer list, we assume the corresponding TACO prediction to be
351 negative. We observed that TICA has a 3-fold higher recall with respect to TACO on the 378
352 candidate list, with only 13% less specificity, resulting in a 1.6-fold increase in geometric mean
353 performance.

354 We then selected 10 highly-conserved TFs from the list of ENCODE ChIP-Seq data available for
355 HepG2 and submitted them to CENTDIST. Feeding the list of TFs and their CENTDIST-predicted
356 partners to TICA resulted in 406 candidate predictions. It is of note that due to the assumptions and

357 target heterotypic interactions, homotypic predictions in CENTDIST positive counts are not
358 considered. As shown in Table 4, TICA has a much better enrichment ratio than CENTDIST with
359 respect to CORUM/BioGRID, demonstrating better specificity but lower recall. However,
360 comparison of recall rate is biased in favor of CENTDIST, since CENTDIST predictions were used to
361 select the TFs for further consideration. It is also worth mentioning that CORUM complexes and
362 CENTDIST's co-motifs are not cell-line specific; hence some verified CENTDIST-only predictions
363 may be false positives in the cell lines tested.

364 To compare our results with the NMF method [30], we extracted complexes on cell lines GM12878
365 and K562 reported previously (Figure 3 in [31]) and compared with TICA predictions on shared TFs.
366 Validation was done using GeneMANIA [31], a gene network builder based on functional annotations
367 that is used by Giannoupoulou et al. [30]. On GM12878, TICA shows improved recall but reduced
368 specificity, resulting in greater geometric mean performance, but lower enrichment ratio with respect
369 to the databases (Table 4 again); on K562, performance between the two methods with respect to
370 proposed complexes is similar (Table 4). However, there is no report of the full list of predicted
371 complexes [30]; so we expect that the comparison is skewed similarly to the CENTDIST comparison.

372

373 **Discussion**

374 In this study, we reported TICA, a new method for predicting interactions between TFs based on
375 structural and positional information of their binding sites. By exploiting the expressive and
376 distributed nature of the GMQL language together with simple statistics, TICA provides fast
377 combinatorial analysis of interactions between TFs for detecting their potential physical interactions.
378 Its main advantage lies in allowing users to do parallel pre-screening of possible novel interactions.
379 TICA shows high specificity toward the commonly-used protein complexes (> 80%), and thus can be
380 exploited to weed out unlikely interactions.

381 The enrichment ratio of TICA's predictions with respect to CORUM ratio is above 1 in all
382 scenarios, which indicates that it can effectively separate true TF-TF interactions and
383 non-interactions. Of note is the fact that TICA reports fewer TF-TF interaction predictions on healthy
384 cell line GM12878 as opposed to disease cell lines HepG2 and K562. Healthy generally have lower
385 transcriptional activity than cancer cells [27], providing indirect evidence supporting the correctness
386 of the prediction ratio.

387 The right tail size feature in TICA is (to the best of our knowledge) a novel introduction to the
388 field. To investigate the relative impact of this feature, we computed all measures under three
389 alternative conditions: using all four features (baseline scenario), using only the 1000-bp right tail
390 size, and using all other three measures (*i.e.*, without the right tail size). As reported in Table S7,

391 incorporating the right tail size test consistently leads to improved geometric mean performance,
392 irrespective of databases and/or cell lines considered. Using right tail size (with the baseline
393 parameters) alone beats all other three measures in terms of geometric mean performance by a large
394 margin in two out of the three cell lines examined. However, we detected lower database enrichment
395 ratio when using the right tail size test alone compared to the baseline scenario. This might be due to
396 a bias in the comparison: using the baseline P value (0.2) in the right tail size test results in laxer
397 conditions for positive calling with respect to the three way test, leading to better recall but lower
398 class separation power.

399

400 **Novel interactions predicted are confirmed by manual investigation**

401 We extracted lists of novel interactions predicted using TICA on the three aforementioned cell lines:
402 we define an interaction as a novel prediction if evidence for it can be found in CORUM but not in
403 PubMed. The combined support by TICA structural predictions and protein complexes/ functional
404 interaction databases is a strong indicator that these interactions are likely to be real. A full list is
405 provided in Table S8; henceforth we highlight some interesting examples.

406 SIN3A/ TFAP4 in HepG2 is supported by the fact that efficient TFAP4 DNA binding is known to
407 require another bHLH protein (<http://www.genecards.org/cgi-bin/carddisp.pl?gene=TFAP4>) and
408 SIN3A contains paired amphipathic helix (PAH) domains, many of which contain basic regions close
409 to the HLH motif (<http://atlasgeneticsoncology.org/Educ/TFactorsEng.html>). The interaction
410 between CEBPB and NR2F2 in K562 is notable because there is evidence of a connection between
411 these two TFs and the regulation of gonadotropin-releasing hormone (GnRH) [32]. Another
412 interesting prediction is JUN / STAT1 in K562. Although we could not find up-to-date evidence of
413 their interaction *in vitro*, JUN is known to interact with STAT3 [33] and STAT1 binds to its interacting
414 partners at the same or very close to the binding sites of STAT3 [34], suggesting a potential
415 interference scenario where tumour suppressor STAT1 could bind to JUN at STAT3's binding sites
416 and thus prevents the formation of JUN/STAT3 complexes in tumor cells. This speculation is
417 supported by evidence of upregulation of c-JUN in mice with knocked-down STAT1 [35]. Finally,
418 evidence has been found that cells transduced with a C-terminally truncated Runx1, which lacks
419 important cofactor interacting sites, showed increased transcription of c-Myc [36], supporting the
420 prediction of MYC / RUNX1 in K562.

421

422 **Taking the union of multiple predictors leads to increased performance.**

423 Based on the comparison discussed in Results, we speculate that taking the union of TICA and TACO
424 or CENTDIST in a given cell might produce an overall improved performance. To validate this

425 possibility, we computed quality measures on the predictions resulting from taking the union of
426 positive predictions from TICA and TACO or CENTDIST (Table 4). We notice a moderate drop in
427 specificity (expected due to taking the union of two predictors) which is balanced by a sizeable
428 increase in recall, leading to an overall increase in geometric mean performance and enrichment ratio,
429 supporting our hypothesis.

430

431 **Conclusions**

432 TICA is a novel methodology that employs genomic positional information of TFBSs to predict
433 physical interactions between TFs. The main advantages of TICA are three-fold. (1) TICA leverages
434 novel, parallel computing techniques to efficiently scan ChIP-seq point-source (1bp-sized) binding
435 site datasets and extract high-confidence binding sites and active TSSs. (2) TICA does not require
436 motif information for TFBSs, bypassing incompleteness of selected motif databases and related
437 accuracy issues. (3) TICA demonstrates very high level of specificity even at the laxest levels of
438 parameters, allowing users to weed out non-interacting TF-TF pairs with high levels of confidence
439 before proceeding to experimental validation.

440 TICA has shown to be as reliable if not better than similar interaction prediction algorithms that
441 rely on precise motif information, while allowing for significantly higher output rates (ranging 5000–
442 22,000 predictions on available cell lines). Moreover, TICA appears complementary to alternative
443 TF-TF interaction prediction approaches (viz., TACO and CENTDIST), and combining their
444 predictions greatly improves sensitivity of the predictions at moderately-reduced specificity.

445 Finally, selected TF-TF pairs could be competing for the same cognate genes and interaction
446 partners (competitive interactors) instead of being part of the same complex (cooperative interactors)
447 Both interactions are interesting in the domain of gene expression regulation, and we plan to address
448 their classification in future studies.

449

450 **Authors' contributions**

451 SP designed the TICA methodology and analyzed the data. PP contributed to the algorithm's
452 construction and performed the code optimization. SC participated in the study design and result
453 validation. LW conceived the study, contributed to the design of TICA, and validated the results. SP
454 drafted the manuscript. All authors reviewed and approved the final manuscript.

455

456 **Competing interests**

457 The authors have declared no competing interests.

458

459 **Acknowledgments**

460 This work was supported by the European Research Council (ERC) Advanced Grant *GeCo*
461 (Data-Driven Genomic Computing; Grant No. 693174) awarded to SC. We would like to thank
462 members of the GeCo project for helpful insights. LW was supported in part by a
463 Kwan-Im-Thong-Hood-Cho-Temple chair professorship and in part by a tier-1 grant (Grant No.
464 MOE T1 251RES1725) from the Ministry of Education, Singapore.

465

466 **References**

- 467 [1] Hughes TR. A handbook of transcription factors. Berlin: Springer Netherlands; 2011.
- 468 [2] Weirauch MT, Hughes TR. A catalogue of eukaryotic transcription factor types, their
469 evolutionary origin, and species distribution. In: Hughes TR, editor. A handbook of
470 transcription factors. Berlin: Springer Netherlands; 2011,p.26–73.
- 471 [3] Zhang Y, Dakic A, Chen R, Dai Y, Schlegel R, Liu X. Direct HPV E6/Myc interactions induce
472 histone modifications, Pol II phosphorylation, and *hTERT* promoter activation. *Oncotarget*
473 2017;8:96323–39.
- 474 [4] Zhang Z, Hu X, Zhang Y, Miao Z, Xie C, Meng X, et al. Opposing control by transcription
475 factors MYB61 and MYB3 increases freezing tolerance by relieving c-repeat binding factor
476 suppression. *Plant Physiol* 2016;172:1306–23.
- 477 [5] Jolma A, Yin Y, Nitta KR, Dave K, Popov A, Taipale M, et al. DNA-dependent formation of
478 transcription factor pairs alters their binding specificity. *Nature* 2015;527:384–9.
- 479 [6] Smale ST. Core promoters: active contributors to combinatorial gene regulation. *Genes Dev*
480 2001;15:2503–8.
- 481 [7] Odom, Duncan T. Identification of transcription factor-DNA interactions *in vivo*. *Subcell*
482 *Biochem* 2011;52:175–91.
- 483 [8] Masseroli M, Pinoli P, Venco F, Kaitoua A, Jalili V, Palluzzi F, et al. Genometric query
484 language: a novel approach to large-scale genomic data management. *Bioinformatics*
485 2015;31:1881–8.
- 486 [9] McKinney W. Data structures for statistical computing in python. *Proc 9th Python Sci Conf*
487 2010;51–6.
- 488 [10] Walt SVD, Colbert SC, Varoquaux G. The NumPy array: a structure for efficient numerical
489 computation. *Comput Sci Eng* 2017;12:22–30.
- 490 [11] Jones E, Oliphant E, Peterson P. *SciPy: open source scientific tools for python*. 2001.
- 491 [12] Geisel N, Gerland U. Physical limits on cooperative protein-DNA binding and the kinetics of
492 combinatorial transcription regulation. *Biophys J* 2011;101:1569–79.
- 493 [13] Crocker J, Abe N, Rinaldi L, McGregor AP, Frankel N, Wang S, et al. Low affinity binding
494 site clusters confer Hox specificity and regulatory robustness. *Cell* 2015;160:191–203.
- 495 [14] Wiesner T, Lee W, Obenauf AC, Ran L, Murali R, Zhang QF, et al. Alternative transcription
496 initiation leads to expression of a novel *ALK* isoform in cancer. *Nature* 2015;526:453–7.
- 497 [15] Arner E, Daub CO, Vitting-Seerup K, Andersson R, Lilje B, Drabløs F, et al. Transcribed
498 enhancers lead waves of coordinated transcription in transitioning mammalian cells. *Science*
499 2015;347:1010–4.

- 500 [16] Sloan CA, Chan ET, Davidson JM, Malladi VS, Strattan JS, Hitz BC, et al. ENCODE data at
501 the ENCODE portal. *Nucleic Acid Res* 2016;44:D726–32.
- 502 [17] Singer M, Kosti I, Pachter L, Mandel-Gutfreund Y. A diverse epigenetic landscape at human
503 exons with implication for expression. *Nucleic Acid Res* 2015;43:3498–508.
- 504 [18] Karnuta JM, Scacheri PC. Enhancers: bridging the gap between gene control and human
505 disease. *Hum Mol Genet* 2018;27:R219–27.
- 506 [19] Du Y, Liu Z, Cao X, Chen X, Chen Z, Zhang X, et al. Nucleosome eviction along with
507 H3K9ac deposition enhances Sox2 binding during human neuroectodermal commitment. *Cell*
508 *Death Differ* 2017;24:1121–31.
- 509 [20] Yu, X, Lin J, Zack DJ, Qian J. Computational analysis of tissue-specific combinatorial gene
510 regulation: predicting interaction between transcription factors in human tissues. *Nucleic*
511 *Acids Res* 2006;34:4925–36.
- 512 [21] Koudritsky M, Domany E. Positional distribution of human transcription factor binding sites.
513 *Nucleic Acids Res* 2008;36:6795–805.
- 514 [22] Jankowski A, Szczurek E, Jauch R, Tiuryn J, Prabhakar S. Comprehensive prediction in 78
515 human cell lines reveals rigidity and compactness of transcription factor dimers. *Genome*
516 *Res* 2013;23:1307–18.
- 517 [23] Jankowski A, Prabhakar S, Tiuryn J. TACO: a general-purpose tool for predicting
518 cell-type-specific transcription factor dimers. *BMC Genomics* 2014;15:208.
- 519 [24] Ruepp A, Waegele B, Lechner M, Brauner B, Dunger-Kaltenbach I, Fobo G. CORUM: the
520 comprehensive resource of mammalian protein complexes—2009. *Nucleic Acid Res*
521 2010;38:D497–501.
- 522 [25] Chatr-Aryamontri A, Oughtred R, Boucher L, Rust J, Chang C, Kolas NK, et al. The
523 BioGRID interaction database: 2017 update. *Nucleic Acids Res* 2017;45:D369–79.
- 524 [26] Batuwita R, Palade V. Adjusted geometric-mean: a novel performance measure for
525 imbalanced bioinformatics datasets learning. *J Bioinform Comput Biol* 2012;10:1250003.
- 526 [27] Kotsantis P, Silva LM, Irscher S, Jones RM, Folkes L, Gromak N, et al. Increased global
527 transcription activity as a mechanism of replication stress in cancer. *Nat Commun*
528 2016;7:13087.
- 529 [28] Ravasi T, Suzuki H, Cannistraci CV, Katayama S, Bajic VB, Tan K, et al. An atlas of
530 combinatorial transcriptional regulation in mouse and man. *Cell* 2010;140:744–52.
- 531 [29] Zhang Z, Chang CW, Goh WL, Sung WK, Cheung E. CENTDIST: discovery of
532 co-associated factors by motif distribution. *Nucleic Acids Res* 2011;39:W391–9.
- 533 [30] Giannopoulou E, Elemento O. Inferring chromatin-bound protein complexes from
534 genome-wide binding assays. *Genome Res* 2013;23:1295–306.
- 535 [31] Warde-Farley D, Donaldson SL, Comes O, Zuberi K, Badrawi R, Chao P, et al. The
536 GeneMANIA prediction server: biological network integration for gene prioritization and
537 predicting gene function. *Nucleic Acid Res* 2010;38:W214–20.
- 538 [32] Gillespie JM, Roy D, Cui H, Belsham DD. Repression of gonadotropin-releasing hormone
539 (GnRH) gene expression by melatonin may involve transcription factors COUP-TFI and
540 C/EBP beta binding at the GnRH enhancer. *Neuroendocrinology* 2004;79:63–72.
- 541 [33] Trierweiler C, Hockenjos B, Zatloukal K, Thimme R, Blum HE, Wagner EF, et al. The
542 transcription factor c-JUN/AP-1 promotes HBV-related liver tumorigenesis in mice. *Cell*
543 *Death Differ* 2016;23:576–82

- 544 [34] Friedrich K, Dolznig H, Han X, Moriggl R. Steering of carcinoma progression by the
545 YIN/YANG interaction of STAT1/STAT. *Biosci Trends* 2017;11:1–8.
- 546 [35] Levano S, Bodmer D. Loss of STAT1 protects hair cells from ototoxicity through modulation
547 of STAT3, c-Jun, Akt, and autophagy factors. *Cell Death Dis* 2015;6:e2019
- 548 [36] Jacobs PT, Cao L, Samon JB, Kane CA, Hedblom EE, Bowcock A, et al. Runx transcription
549 factors repress human and murine c-Myc expression in a DNA-binding and C-terminally
550 dependent manner. *PLoS One* 2013;8:e69083.

551

552 **Figure legends**

553 **Figure 1 Example of mindist couple extraction on synthetic TFBS data**

554 The closest binding site fitting the criteria becomes paired with the anchor and forms a mindist
555 couple, and their distance is defined as the couple distance accordingly. If both the adjacent binding
556 sites are valid and tied for the closest, two different mindist couples with identical distance values
557 are generated. If none of the two is valid, no couple is generated and the algorithm then proceeds to
558 the next binding site. Note that a single binding site does not have to belong to only one couple, but
559 any couple formed by the exact same binding sites (in any order) is only counted once. **A.** The TF2
560 binding sites (yellow) can only be associated to the first TF1 sample (blue), as the next one in the
561 sorting has the same label. **B.** and **C.** TF1 is associated to both TF2 sites. These couples are found
562 twice but only counted once. **D.** One of the two TF2 sites is out of admissible range for the TF1 site,
563 so only one couple is found. **E.** and **F.** Both TF1 sites are equally distant to the anchor TF2 site, both
564 generate a mindist couple.

565

566 **Figure 2 Histograms of distance distribution for TF couple CTCF and Myc in HepG2**

567 **A.** Distance distribution of the TF couple for CTCF and Myc, for which there is no evidence known
568 to support the interaction behavior. **B.** Zoomed view of the distribution short and long tails. In both
569 panels, blue columns denote the head of the distribution (couples with distance ranging 0–500 bp),
570 red columns denote the short right tail of the distribution (distance > 1000 bp), and orange columns
571 denote the long right tail of the distribution (distance > 500 bp). Note that the 500-bp tail and
572 1000-bp tail overlap for the distances > 1000 bp. CTCF: CCCTC-binding factor.

573

574 **Figure 3 Histograms of distance distribution for TF couple MAX and Myc in HepG2**

575 **A.** Distance distribution of the TF couple for MAX and Myc, which are well-known interacting TFs.
576 **B.** Zoomed view of the distribution short and long tails. In both panels, blue columns denote the
577 head of the distribution (couples with distance ranging 0–500 bp), red columns denote the short
578 right tail of the distributions (distance > 1000 bp), and orange columns denote the long right tail of
579 the distribution (distance > 500 bp). Note that the 500-bp tail and 1000-bp tail overlap for the

580 distances > 1000 bp. MAX, Myc-associated factor X.

581

582 **Figure 4 Mindist couple distance right tails using TFs ARID3A and ATF1 on cell line HepG2**

583 Blue columns denote the head of the distributions, red columns denote the short right tail of
584 distribution (distance > 1000 bp) and orange columns denote the long right tail of the distribution
585 (distance > 500 bp). Note that the 500-bp tail and 1000-bp tail overlap for the distances > 1000 bp.

586

587 **Figure 5 Summary of positive predictions supported by the literature**

588 **A.** Literature analysis of the positive predictions for cell line HepG2. A positive prediction can be
589 “Verified as POS” if interaction evidence is found in published literature (green); “Verified as NEG”
590 if evidence is found that there is no interaction between members (red); or it can be “Unverified” if
591 no evidence is found for either case (blue). **B.** Database cross-check of verified positive predictions
592 for cell line HepG2. “Not in any database” (red) means that the predicted interactions are not found
593 in either CORUM or BioGRID; blue indicates the number of positive predictions not found in
594 BioGRID, whereas orange indicate the number of positive predictions not found in CORUM. Green
595 slice indicates the number of predictions found in at least one of the two databases. **C.** Positive
596 predictions literature analysis for cell line K562 (same color code as A). **D.** Database cross-check of
597 verified positive predictions for cell line K562 (same color code as B). *pred.:* predictions.

598

599 **Tables**

600 **Table 1 List of TICA parameters and values used in this study**

601

602 **Table 2 Dataset cardinalities for all cell lines used in TICA computational**
603 **experiments**

604

605 **Table 3 Cross-cell line comparison of positive TICA predictions**

606

607 **Table 4 Comparison between TICA, TACO, CENTDIST, and NMF predictions**

608

609 **Supplementary material**

610 **File S1 GMQL queries for TICA data extraction and preprocessing**

611

612 **File S2 Additional discussion on validation and *P* value threshold selection**

613

614 **Table S1 List of predictions with manual literature investigation performed**
615
616 **Table S2 Quality measures for TICA predictions with respect to CORUM and BioGRID**
617 **databases**
618
619 **Table S3 Background TFs and candidate listings for all cell lines in TICA computational**
620 **experiments**
621
622 **Table S4 TICA interaction predictions**
623
624 **Table S5 Literature validation of TICA predictions in cell lines HepG2 and K562**
625
626 **Table S6 TF–TF interaction predictions conserved across various cell lines examined**
627
628 **Table S7 Prediction quality measures relative to right tail size test for all cell lines**
629
630 **Table S8 Novel TF–TF predictions with confirmation from CORUM and/or BioGRID**

Figure 1
[Click here to download high resolution image](#)

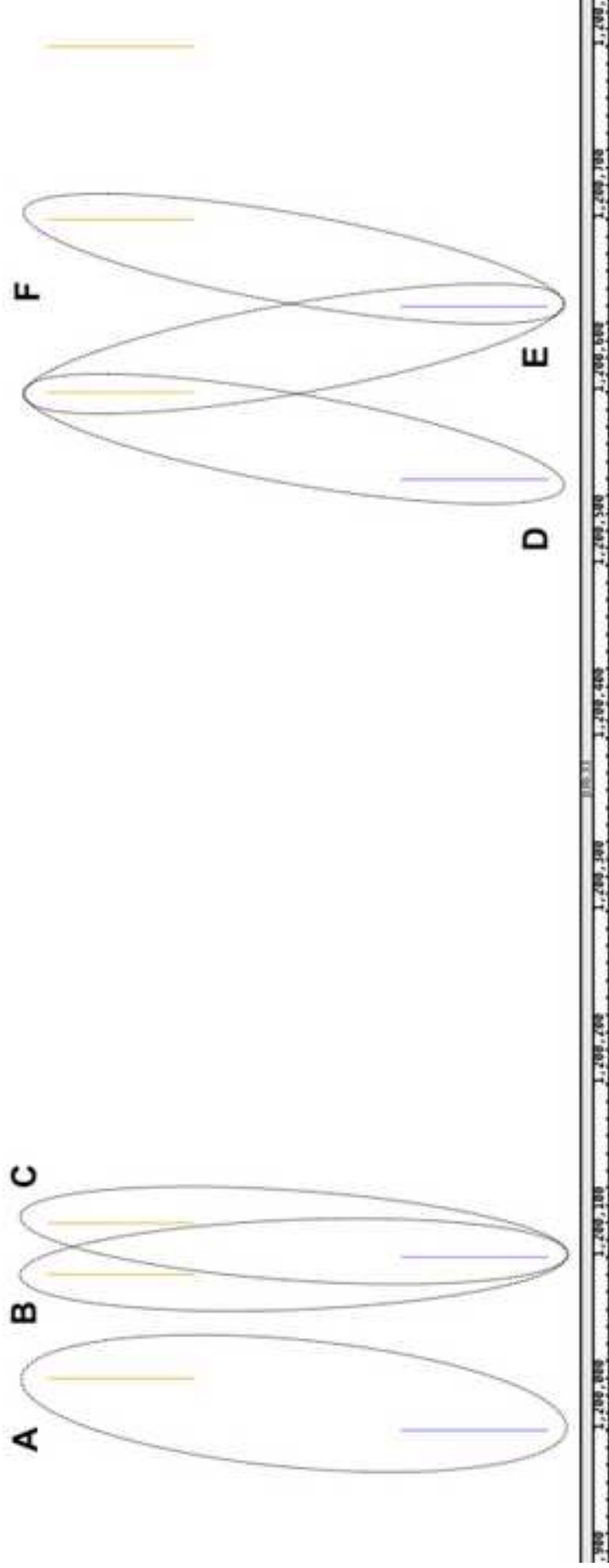
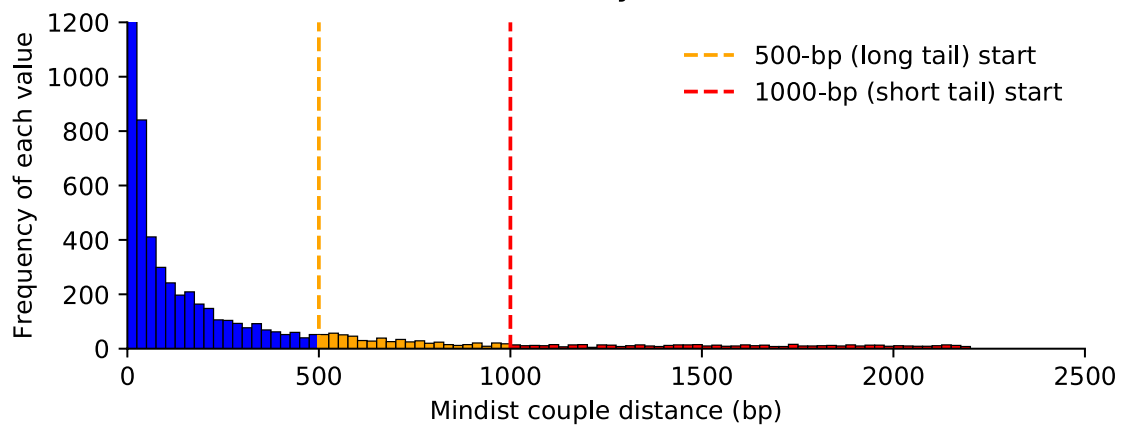


Figure 2

A Full distance distribution for CTCF and Myc



B Distance distribution tail for CTCF and Myc

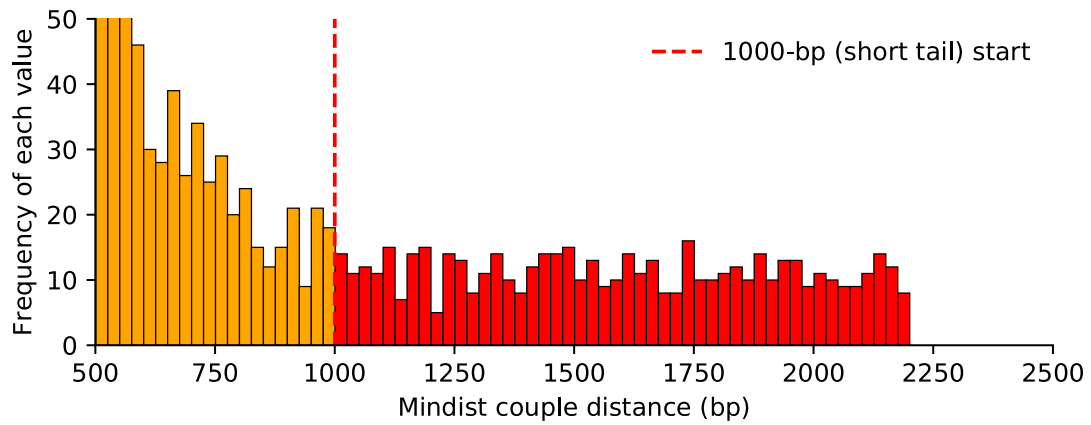
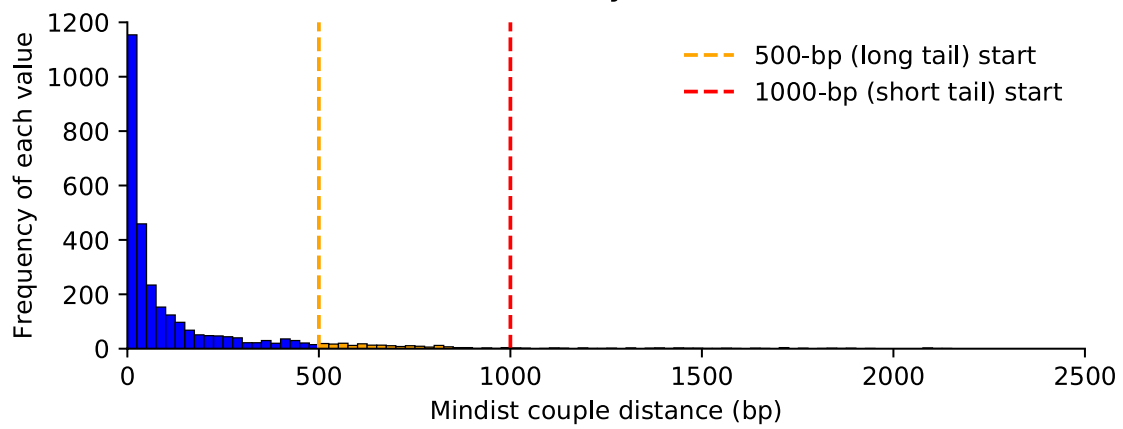


Figure 3

A Full distance distribution for MAX and Myc



B Distance distribution tail for MAX and Myc

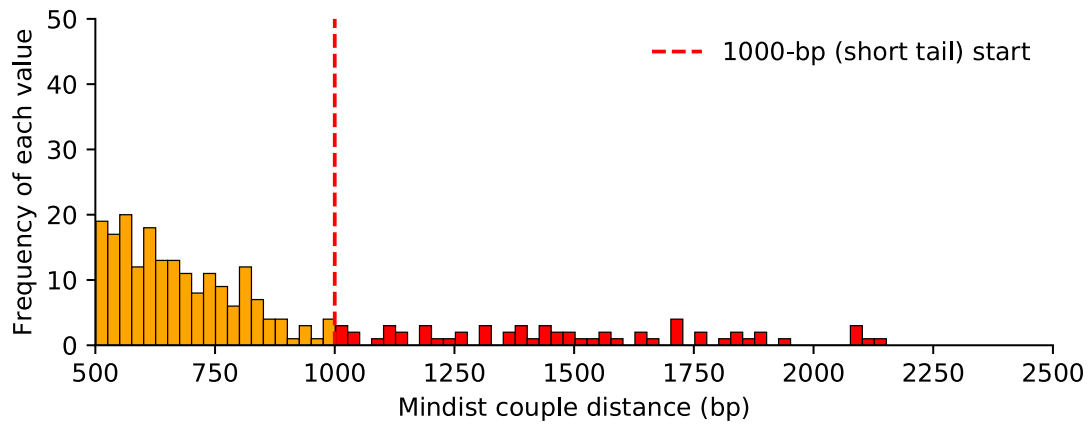


Figure 4

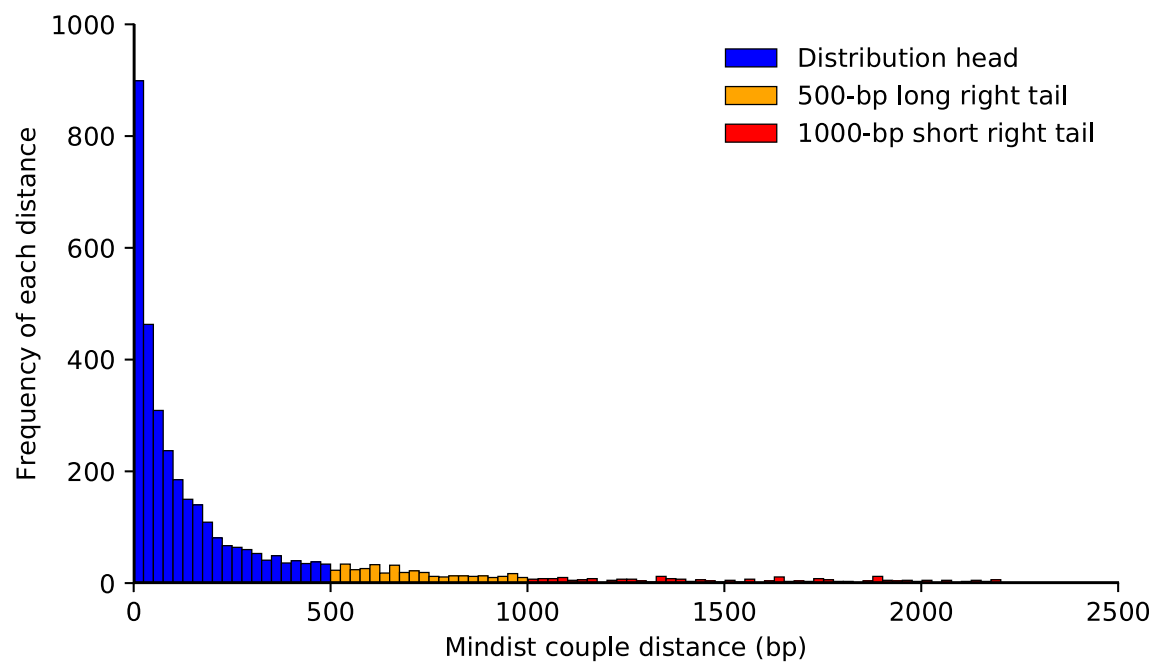


Figure 5

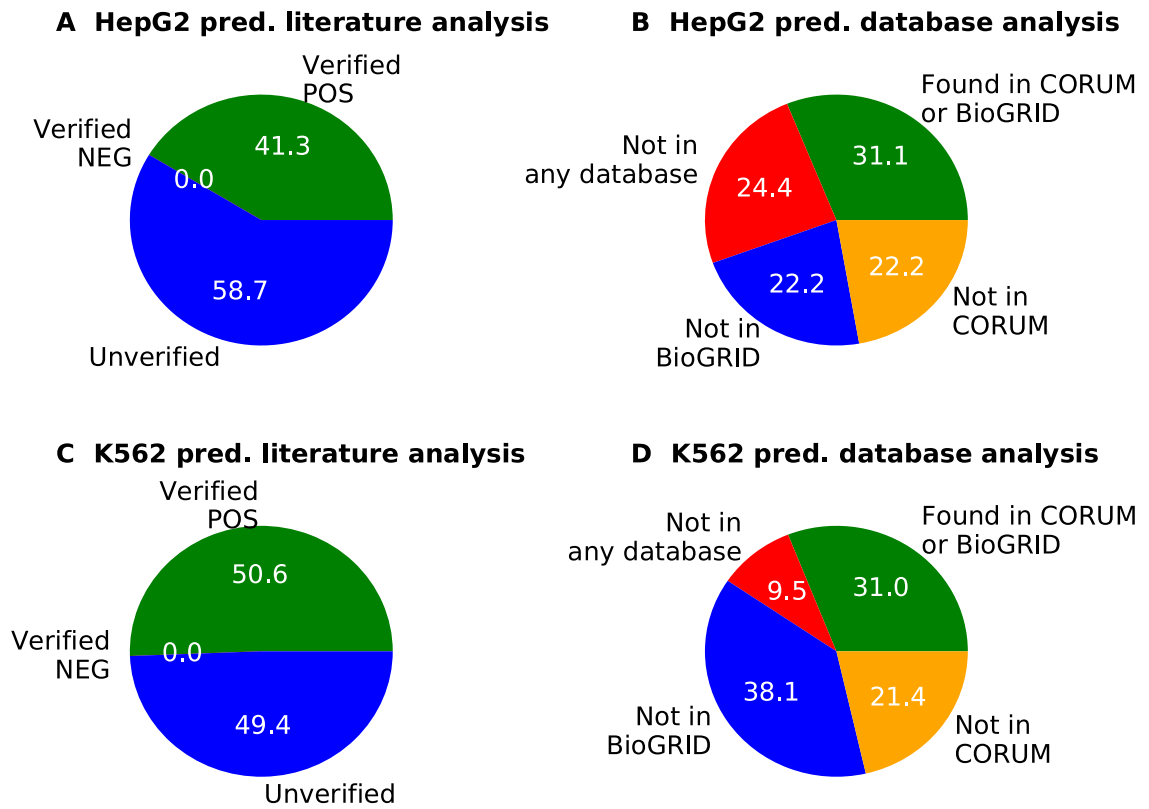


Table 1 List of TICA parameters and related values

Class	Parameter	Chosen value	Category
Genomic dimensions	Gene body length	200 bp	Nominal
	Promoter length	2000 bp	Nominal
Metric constraints	Mindist couple max distance	2200	Computed
Tests and thresholds	Number of points in nulls	10,000	Tuned
	Test <i>P</i> value	0.2	Tuned
	Required number of rejected null hypotheses	1	Nominal
	Minimum number of mindist couples	1	Tuned
	Minimum fraction of mindist couples collocating in a shared promoter	0.01	Tuned

Note: Parameters are classified as nominal, tuned or computed. Nominal values are chosen as standard or reference while tuned values are set according to data analysis methods. The computed mindist couple max distance is defined to be the sum of one standardized promoter length and one standardized gene body length.

Table 2 Dataset cardinalities for all cell lines used in TICA computational experiments

Cell line	No. of available TFs	Total size (after filtering)	No. of active TSSs
HepG2	103	2.95 Gb	97,904
GM12878	102	6.4 Gb	122,854
K562	214	1.9 7Gb	59,556

Note: Data are obtained from ENCODE phase 2 and 3 database, narrowPeak format. TSS, transcription start site.

Table 3 Cross-cell comparison of positive TICA predictions

Cell line1	Cell line 2	Positive predictions on shared TFs	Jaccard coefficient	Recall in cell line 1	Recall in cell line 2
HepG2	GM12878	46	0.146	0.177	0.426
HepG2	K562	89	0.163	0.256	0.309
GM12878	K562	110	0.186	0.460	0.237
HepG2	GM12878 \cup K562	121	0.191	0.111	0.210
GM12878	HepG2 \cup K562	142	0.186	0.181	0.276
K562	HepG2 \cup GM12878	185	0.192	0.079	0.645
All cell lines (intersection)		14	0.186	0.089 / 0.206 / 0.130	

Note: For the intersection of all three cell lines, the recall value is given for all cell lines, in order (*viz.*, recall with respect to HepG2, GM12878, and K562). For comparisons involving all three cell lines, a TF in a prediction must be shared between all cell lines in order for it to be accepted as part of the combination / intersection.

Table 4 Comparison between TICA, TACO, CENTDIST, and NMF predictions

Predictor	Cell line	Recall	Specificity	Geometric mean performance	Enrichment
TICA	K562	0.421	0.807	0.583	2.181
TACO	K562	0.140	0.938	0.362	2.258
TICA \cup TACO	K562	0.526	0.760	0.632	2.192
TICA	HepG2	0.278	0.857	0.488	1.944
CENTDIST	HepG2	0.390	0.720	0.530	1.393
TICA \cup CENTDIST	HepG2	0.585	0.643	0.613	1.639
TICA	GM12878	0.424	0.611	0.509	NA*
NMF	GM12878	0.238	0.911	0.468	NA*
TICA	K562 [#]	0.202	0.792	0.400	NA*
NMF	K562	0.214	0.835	0.423	NA*

Note: Union of predictors is defined as predicting a positive interaction if and only if it is predicted positive by at least one of TICA and TACO/CENTDIST (respectively). An interaction is predicted negative if and only if it is predicted negative by both methods. Comparison was performed only on the cell lines indicated (K562 for TACO, HepG2 for CENTDIST, GM12878, and K562 for NMF [23]). * indicates that there is no software available for database-wide comparison; # indicates that only a subset of TFs predicted by NMF to be in complexes are used for comparison. NMF, nonnegative matrix factorization method by Giannopoulou and colleagues [30].